Neutron Scattering Study of Segmental Dynamics in the Disordered Regions of Partially Crystalline Polyethylene

G. Hohlweg,† B. Holzer,† W. Petry,‡ G. Strobl,*,‡ and B. Stühn†

Fakultät für Physik, Universität Freiburg, 7800 Freiburg, Germany, and ILL, Grenoble, France

Received March 25, 1992; Revised Manuscript Received July 20, 1992

ABSTRACT: Segmental dynamics in the disordered regions of partially crystalline polyethylene was investigated by quasielastic incoherent neutron scattering. Experiments provide evidence for the peculiar nature of the disorderd regions, where the motion is restricted due to the chain fixing in the crystallites and the unresolvable entanglements. There are strong variations in the mobility between different samples. Partial melting results in a release of the constraints, which is reflected in an increase in the mobility. Conclusions are based on a determination of the mean-squared displacements $\langle u^2 \rangle_r$ in all the disordered regions. Values for $\langle u^2 \rangle_r$ were derived from T- and q-dependent elastic window scans and measured dynamic structure factors. In the frequency range of the experiment motion is made up of two components, the fast local mode generally found in glass-forming liquids and a slow diffusive mode which corresponds to the β- and γ-process. Up to the onset of partial melting they contribute with similar weights to $\langle u^2 \rangle_r$. Partial melting then mainly affects the slow diffusive mode and leads to a further increase of its amplitude.

Introduction

Segmental motion in the disordered regions of partially crystalline polymers is different from that in a pure melt. Due to the fixing of part of the macromolecules in the adjacent crystallites the motion remains spatially confined; a free diffusion cannot occur. Further limitations follow from the presence of the entanglements, which here are unresolvable. There are also indications for a strong enhancement of the entanglement density compared to a pure melt. One usually observes a continuous decrease of the thickness of the amorphous layers during cooling,[1,2] which is necessarily associated with a corresponding increase in the entanglement density. Hence, the structure of the disordered layers in partially crystalline polymers has a specific character and one can expect effects on the molecular dynamics.

We have investigated the dynamics by incoherent quasielastic neutron scattering experiments on polyethylene. Measurements were performed on samples with different partially crystalline structure, obtained by crystallization from solution or the melt. Experiments were conducted as a function of temperature, from 130 K up to the crystallite melting point. Information on the dynamics was derived from fixed-window temperature scans and from selectively determined full spectra, both obtained by use of back-scattering spectrometers.

Data evaluation yields the mean-squared displacements of the protons in the crystalline and amorphous regions as a function of temperature. One observes pronounced differences in the segmental mobility in the amorphous layers between the different samples. The temperature dependence reflects the glass transition and the onset of surface melting of the crystallites. Evaluation of the full spectra enables a characterization of the modes of motion which contribute to the displacements.

Experimental Part

Three different samples were investigated: sample I, a linear polyethylene with ultrahigh molecular weight ($M > 10^6$) crystallized at 85 °C from a dilute (0.1%) xylene solution (then washed with methanol and dried under vacuum at 25 °C); sample II, the same compound, melt-crystallized at 125 °C; sample III, a branched low-density polyethylene (33 CH_3/1000 C), crystallized by slow cooling from 160 °C to room temperature (3-h cooling time). The linear polyethylene was a product of Hoechst AG (GUR) and the branched polyethylene a product of BASF AG (Lupolen 1800 S). The crystallinities, as determined by DSC, were 83%, 67%, and 50% for samples I–III, respectively.

The continuous melting of the samples during heating was analyzed by Raman spectroscopy, in order to obtain values independent from the neutron scattering experiment. Raman spectra were registered using a Coderg T800 spectrometer together with an Ar laser.

The neutron scattering experiments were conducted at the Institut Laue-Langevin, Grenoble, France. We used two back-scattering spectrometers which differed in energy resolution, δE, and energy and momentum transfer, ΔE and q:

$$\text{IN10:}\quad \delta E = 1\ \mu\text{eV},\ \Delta E < 15\ \mu\text{eV},\ q < 2\ \text{Å}^{-1}$$

$$\text{IN13:}\quad \delta E = 8\ \mu\text{eV (2 GHz)},\ \Delta E < 200\ \mu\text{eV},\ q < 5\ \text{Å}^{-1}$$

First, fixed-window temperature scans were conducted, yielding the temperature dependence of the intensity $S_0(q)$ in the elastic channel. Here only those neutrons are counted, which changes their energy by an amount less than δE. Then, in a second part, complete quasielastic spectra were registered for the branched and the solution-crystallized linear polyethylene at some selected temperatures. The measured data were corrected for the background scattering and were normalized by referring them to a low-temperature measurement at 100 K. At this lowest temperature only oscillatory motions exist. They were accounted for by an addition of the corresponding mean-squared displacement $\langle u^2 \rangle$ (T = 100 K). The value $\langle u^2 \rangle$ (100 K) was determined in a separate measurement using a vanadium sample for calibration. We found $\langle u^2 \rangle$ (100 K) = 0.03 and 0.06 Å^2 for sample I and samples II and III, respectively. Measurements were performed on films with a thickness of 0.1 mm which were placed in a cylindrical sample holder made of aluminum. For this sample form multiple scattering effects become negligible.

Fixed-Window Scans

Method of Analysis. Polyethylene scatters neutrons essentially incoherently. For the partially crystalline systems under study motion remains confined. Assuming a Gaussian distribution of the displacements, as they follow from the superimposed oscillatory and diffusive motions, the motion leads to a decrease of the elastic incoherent

* Author to whom correspondence should be addressed.
† Universität Freiburg.
‡ ILL.

0024-9297/92/2225-6248$03.00/0

structure factor given by[3]

$$S^{inc}(q,\omega=0) = \sigma^{inc} \exp[-(\langle u^2\rangle q^2/3)] \quad (1)$$

Here σ^{inc} denotes the cross section for incoherent scattering of the fixed protons. The intensity decrease due to the motion is described by a Debye–Waller factor, which includes as the only parameter the mean-squared displacement $\langle u^2\rangle$.

The data presented in the following were obtained using an elastic window (index "0") with limited energy resolution δE and were normalized with regard to the measurement at the lowest temperature, T_{min}:

$$\tilde{S}_0(q;T) = S_0^{inc}(q;T)/S_0^{inc}(q;T_{min}) \quad (2)$$

The structure of the samples can be approximately described by a two-phase model, being composed of crystalline and disordered regions with fractions α and $1-\alpha$. Correspondingly, $\tilde{S}_0(q)$ is set up by two components with different Debye–Waller factors:

$$\tilde{S}_0(q) = \alpha \exp[-(\langle u^2\rangle_c q^2/3)] + (1-\alpha) \exp[-(\langle u^2\rangle_a q^2/3)] \quad (3)$$

At elevated temperatures, where diffusive motions become activated in the amorphous regions, the mean-squared displacement in the amorphous regions, $\langle u^2\rangle_a$, will be larger than that in the crystalline regions, $\langle u^2\rangle_c$. We set

$$\langle u_2\rangle_c = \langle u^2\rangle_v \quad (4)$$

$$\langle u^2\rangle_a = \langle u^2\rangle_v + \langle u^2\rangle_r \quad (5)$$

assuming equal contributions from the vibrations, $\langle u^2\rangle_v$, and an additional contribution in the amorphous phase resulting from relaxatory diffusive motions, $\langle u^2\rangle_r$.

Hence

$$\tilde{S}_0(q) = \exp[-(\langle u^2\rangle_v q^2/3)][\alpha + (1-\alpha) \exp[-(\langle u^2\rangle_r q^2/3)]] \quad (6)$$

Equation 6 was used to derive from the q-dependent elastic window scans by a data fitting the interesting values $\langle u^2\rangle_v(T)$ and $\langle u^2\rangle_r(T)$.

Since the elastic window possesses a finite width (δE), the derived mean-squared displacements $\langle u^2\rangle_r$ are generally smaller than the full displacements following from the diffusive motion. Only those contributions which occur on time scales shorter than the instrumental resolution become effective. $\tilde{S}_0(q)$ therefore does not correspond strictly to the elastic incoherent structure factor, which would enable a precise determination of the spatial extension of the confined motion. Nevertheless, we are dealing with a well-defined quantity. The parameter $\langle u^2\rangle_r$ describes the mean-squared displacement resulting from all diffusive modes with relaxation times shorter than ~1 ns.

Results and Discussion. Figure 1 shows fixed-window scans $\tilde{S}_0(T)$ for three different q's obtained for samples I (a), II (b) and III (c). One observed a continuous decrease with increasing temperature up to a complete vanishing of $\tilde{S}_0$ at the respective crystallite melting points. At temperatures below 200 K the change is linear, but then a stronger decrease sets in in two steps, most clearly shown by the melt-crystallized linear PE (Figure 1b). The second step is obviously related to the onset of melting, surface melting as well as the melting of whole crystallites. The

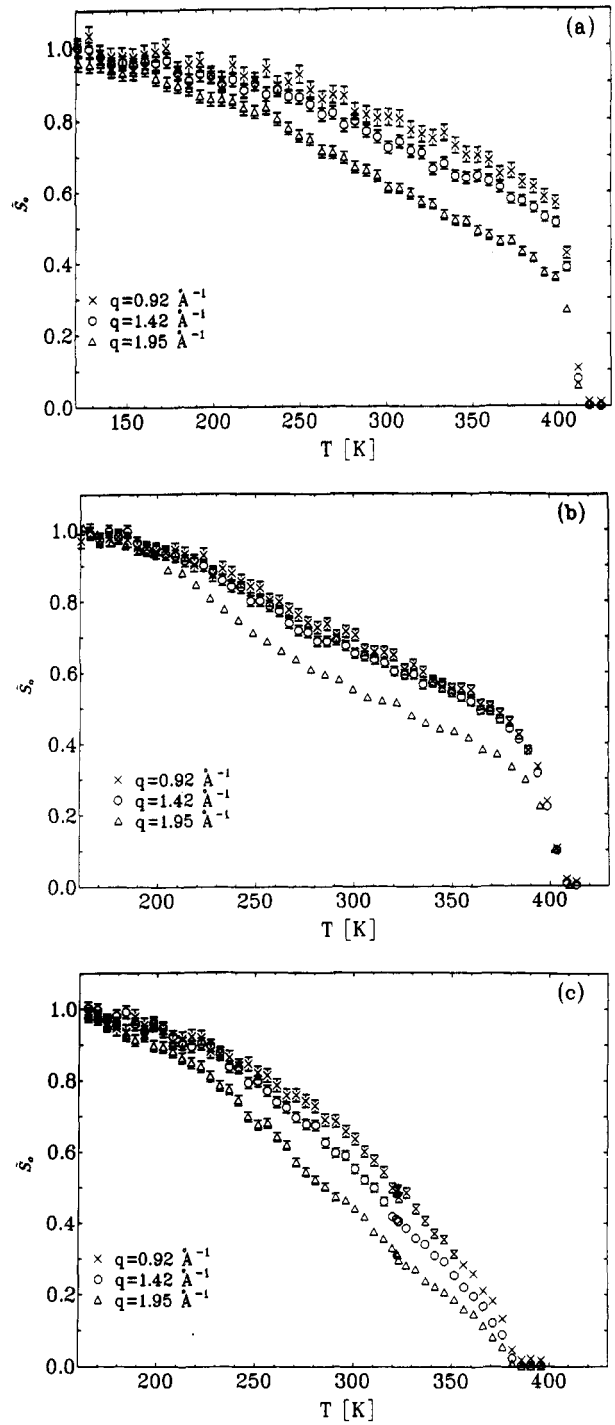

Figure 1. Temperature dependence of the intensity in the elastic window of IN10, measured for the solution-crystallized linear PE (sample I, a), the melt-crystallized linear PE (sample II, b), and the branched PE (sample III, c) at the indicated q's.

first step can be considered as indicating the activation of a specific type of motion with a finite amplitude.

Figure 2a gives the q dependence of $\tilde{S}_0$ for different temperatures, measured for sample I on IN13; Figure 2b shows corresponding curves obtained for sample II on IN10. The curves represent data fits on the basis of eq 6. The fits appear satisfactory and yield the interesting displacements $\langle u^2\rangle_v$ and $\langle u^2\rangle_r$. Usually the analysis was based on measurements on both instruments, IN10 and IN13. The value $\langle u^2\rangle_v$ was determined by the IN13 measurement, which covers a larger q range. Due to the different energy resolution, different values $\langle u^2\rangle_r$ follow in general from the measurements on IN10 and IN13. Regarding the higher q resolution, the data derived from the IN10 measurement appear to be more precise. Figure

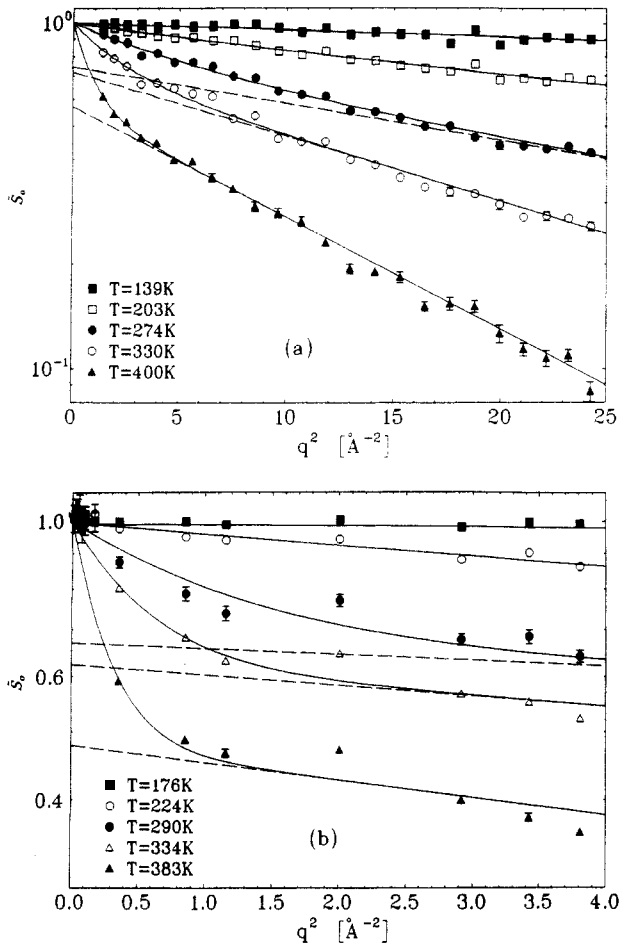

Figure 2. q dependence of the intensity in the elastic window, measured at the indicated temperatures for (a) sample I on IN13 and (b) sample II on IN10. The curves represent fits on the basis of eq 6.

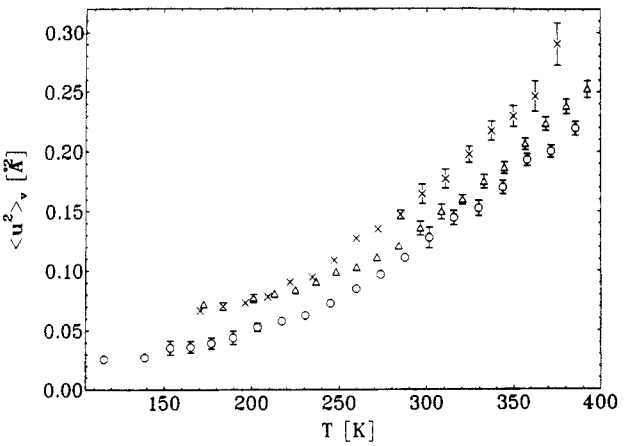

Figure 3. Temperature dependence of the mean-squared vibrational displacements $\langle u^2 \rangle_v$ derived from the elastic window scans on IN13 for samples I (○), II (△), and III (×).

3 shows the vibrational displacements $\langle u^2 \rangle_v$ as they follow from the data evaluation for all three samples; Figure 4 presents the temperature dependences of the relaxatory displacements $\langle u^2 \rangle_r$. One notes differences between the three samples, quite pronounced ones for $\langle u^2 \rangle_r$ and small ones for $\langle u^2 \rangle_v$. Displacements show the lowest values for the solution-crystallized linear PE and the largest values for the branched PE.

The increase in $\langle u^2 \rangle_v$ with temperature is nonlinear, as should be the case for a crystallite with a high thermal expansion coefficient. Displacements are mainly due to the librational motions of the chains about their long axis,

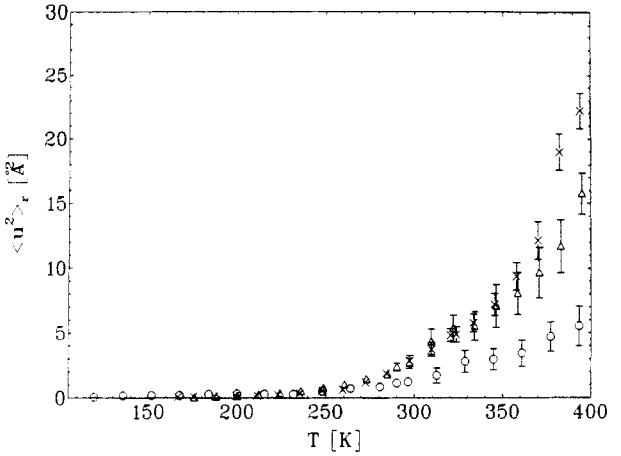

Figure 4. Temperature dependence of the mean-squared relaxatory displacements $\langle u^2 \rangle_r$ derived from the elastic window scans on IN10 for samples I (○), II (△), and III (×).

which show a distinct anharmonicity.[4] The diffusive displacements $\langle u^2 \rangle_r$ become first observable around 230 K, increase in a first step to values of 2 and 5 Å^2 for the solution-crystallized and melt-crystallized samples, respectively, and then increase further beginning at 350 K. This is the behavior which already showed up directly in the fixed-window scans in Figure 1.

The second step is in fact directly related to the onset of melting. In addition to $\langle u^2 \rangle_v(T)$ and $\langle u^2 \rangle_r(T)$ the data evaluation based on eq 6 yields also the temperature dependences of the crystallinity, $\alpha(T)$. Figure 5 shows the results obtained, in a comparison with crystallinity data derived from a decomposition of Raman spectra.[5] Results indicate for the linear PE (samples I and II) an onset of partial melting around 350 K. For the branched PE melting already starts at 280 K. Generally larger crystallinity values are derived from the neutron scattering data. This observation is indicative of the occurrence of disordered regions with low mobility, as they might exist near the crystallite surfaces. In the Raman spectrum these regions contribute to the amorphous band, whereas in the quasielastic neutron spectrum they add to the unresolved "elastic" line.

The important observation is the strong difference in the segmental mobility between the three samples. It provides direct evidence for the specific state of order in the disordered regions of PE. For a phase identical to the pure melt no differences should occur. The experiments indicate a particularly high restriction of the segmental motion in the solution-crystallized sample. These restrictions are much weaker for the branched sample, which possesses the lowest crystallinity. It is also interesting to note that the segmental motion sets in for all samples around 250 K, which is the location of the glass transition for a purely amorphous PE (as can be produced by including counits in sufficient high concentration). Hence, even for the solution-crystallized PE, which exhibits no mechanical relaxation around 250 K, this temperature appears to be a significant one with regard to the segmental motion.

As can be observed, the onset of partial melting leads to an increase in the mobility of all segments in the disordered phase, rather than only to an increase in the number of mobile segments. The continuous surface melting of the crystallites, which is the basis of partial melting, is obviously related to and driven by this increase in the mobility. The observation confirms a basic assumption in theoretical works of Fischer,[6] Zachmann,[7] and Rieger and Mansfield[8] dealing with the process of surface

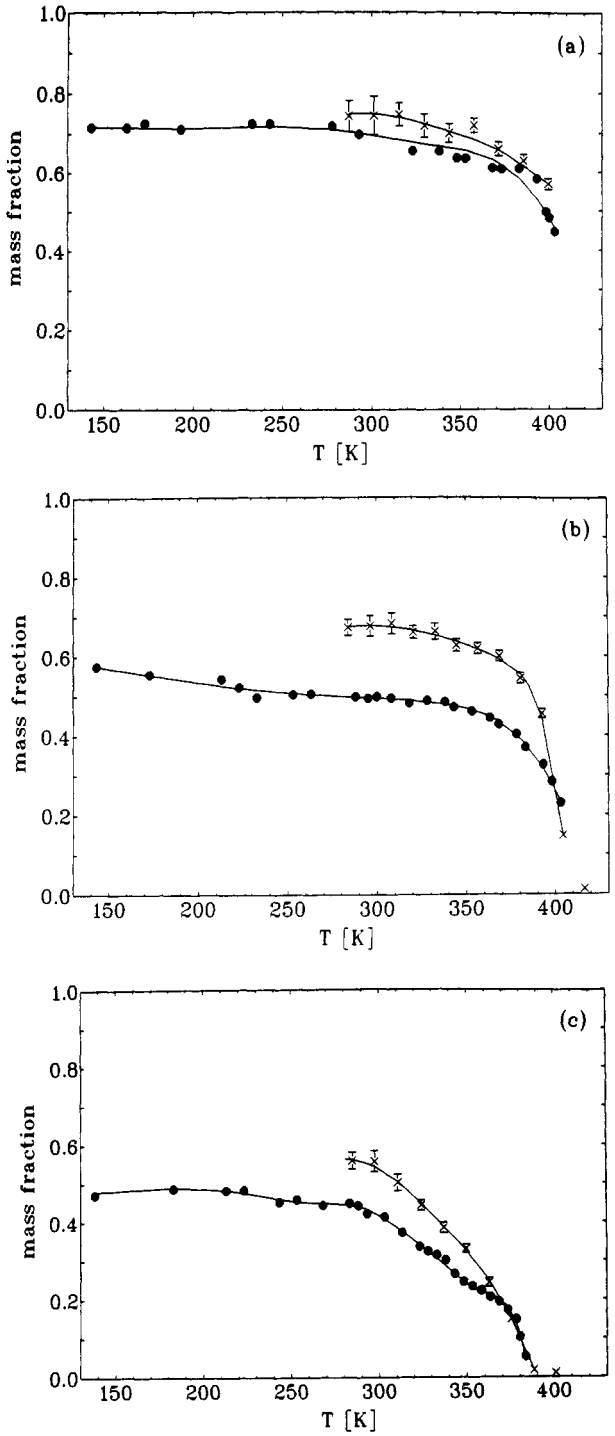

Figure 5. Temperature dependence of the crystallinity of samples I (a), II (b), and III (c). Values derived from the elastic window scans (×) compared to values obtained by Raman spectroscopy (●).

melting. Here surface melting is described as a result of the increasing entropy per monomer if the loops in the amorphous regions become larger. The observed increase in the displacements $\langle u^2 \rangle_r$ at the onset of surface melting demonstrates that this is in fact the case.

Quasielastic Spectra

Results. Spectral Decomposition. In order to characterize the motions which result in the observed diffusive displacements $\langle u^2 \rangle_r$, full quasielastic spectra were registered for some cases of interest. Although this part of the study is not yet complete, due to limitation in the measuring time, it provides valuable insights and can contribute to the basic understanding.

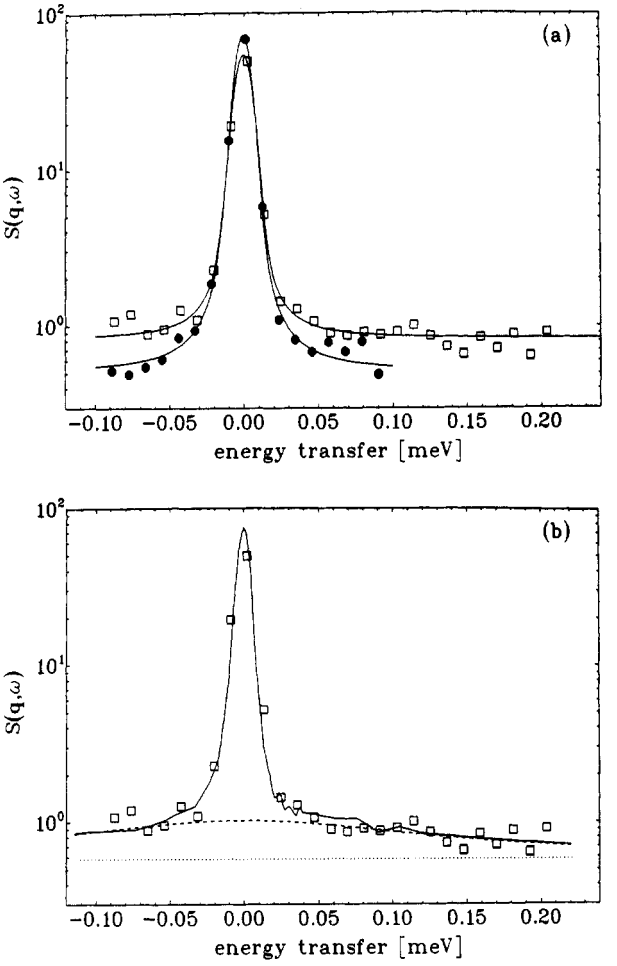

Figure 6. (a) Dynamic structure factor measured on IN13 for sample I at $q = 1.393$ Å^{-1} for $T = 120$ (●) and 350 K (□). (b) Representation of the 350 K data by eq 10.

A first series of quasielastic spectra was measured for the solution-crystallized linear PE using IN13. We performed a measurement at 120 K and further measurements between 350 and 375 K. Figure 6a shows in a comparison the spectra for $q = 1.393$ Å^{-1} registered at 120 and 350 K. One observes a decrease of the elastic intensity associated with an increase of the intensity at higher energy transfers. The low-temperature spectrum corresponds to an unresolved elastic line sitting on a constant background (S_B), convoluted with the (normalized) instrumental resolution function $\phi_{13}(\omega)$

$$S(q,\omega) = S_B + \delta(\omega) \otimes \phi_{13}(\omega) \quad (7)$$

Although the measurement at 350 K does not cover the complete spectrum, an extrapolation to higher values of the energy transfer appears possible. One can make use of the constancy of the integral intensity, which holds if the oscillatory Debye–Waller factor is accounted for:

$$\int S(q,\omega;T{=}120\text{ K})\, d\omega = \int S(q,\omega;T{=}350\text{ K})\, d\omega = 1 \quad (8)$$

with

$$S(q,\omega;T) = S^{inc}(q,\omega;T) \exp(\langle u^2 \rangle_v(T) q^2/3) \quad (9)$$

Figure 6b shows a representation based on eq 8, assuming the following form:

$$S(q,\omega) = \left[S_B + S_E(q)\, \delta(\omega) + S_{L1}(q) \frac{1}{\Pi} \frac{\Gamma_1/2}{\omega^2 + (\Gamma_1/2)^2} \right] \otimes \phi_{13}(\omega) \quad (10)$$

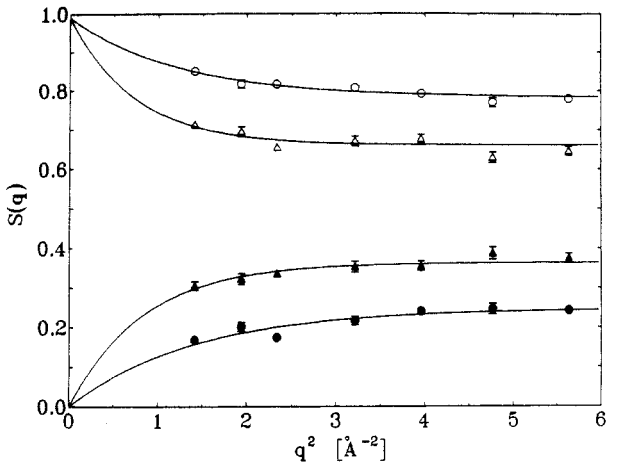

Figure 7. Sample I, T = 350 (●, ○) and 360 K (▲, △). Structure factors associated with the elastic part (open symbols) and the quasielastic part (filled symbols) of the spectrum.

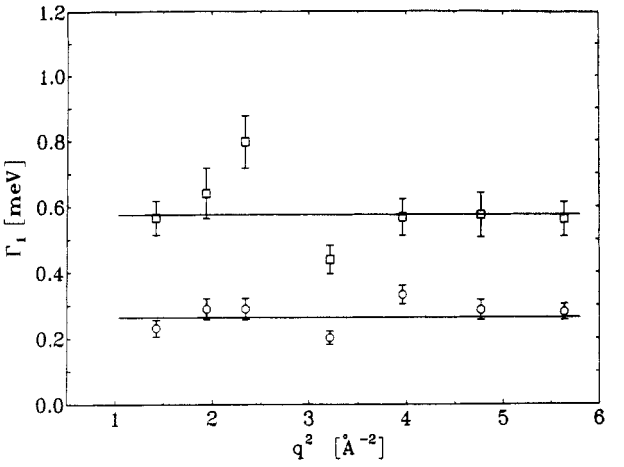

Figure 8. Sample I, T = 350 (○) and 360 K (□). Relaxation rates of the mobile protons as a function of q.

with

$$S_E(q) + S_{L1}(q) = 1$$

Here the dynamic component is given by a Lorentzian with half-width Γ_1, which shows up in addition to an unresolved elastic line. The background S_B is assumed as temperature independent. The data fit yields the static structure factors $S_E(q)$ and $S_{L1}(q)$ associated with the elastic and quasielastic part of the spectrum, as well as the relaxation rate Γ_1. For displacements with a Gaussian distribution one expects

$$S_{L1}(q) = (1 - \alpha)(1 - \exp[-(\langle u^2\rangle_r q^2/3)]) \quad (11)$$

$$S_E(q) = \alpha + (1 - \alpha)\exp[-(\langle u^2\rangle_r q^2/3)] \quad (12)$$

which corresponds in good approximation to eq 6. $S_E(q)$ incudes protons in both the amorphous and the crystalline regions; contributions to $S_{L1}(q)$ originate only from the protons in the disordered regions.

Figure 7 shows the structure factors $S_E(q)$ and $S_{L1}(q)$, as they followed from the fitting of the IN13 data for sample I measured at 350 and 360 K, together with adjusted curves according to eqs 11 and 12. The values derived for the displacements by the curve adjustment are

$$\langle u^2\rangle_r = 2.1\ \text{Å}^2 \quad \text{for } T = 350\ \text{K}$$

$$\langle u^2\rangle_r = 3.9\ \text{Å}^2 \quad \text{for } T = 360\ \text{K}$$

Figure 8 gives the associated relaxation rates. They lie in the range 0.2–0.6 meV. Γ_1 appears to be independent of q and shows an increase going from 350 to 360 K.

A second series of measurements was conducted on IN10, the instrument with the higher resolution but smaller spectral range, for the branched PE (sample III). The instrument enables a detection of a quasielastic line broadening in the μeV range, which was impossible using IN13. The series began with a low-temperature measurement at 100 K, followed by measurements at several temperatures between 250 and 350 K. Figure 9a shows the dynamic structure factor for q = 1.71 Å^{-1}, as obtained at 100 and 320 K. One clearly observes a line broadening in the spectral range of the instrument. Figure 9b gives a representation of the data, which accounts for the obvious occurrence of a quasielastic line in the μeV range in addition

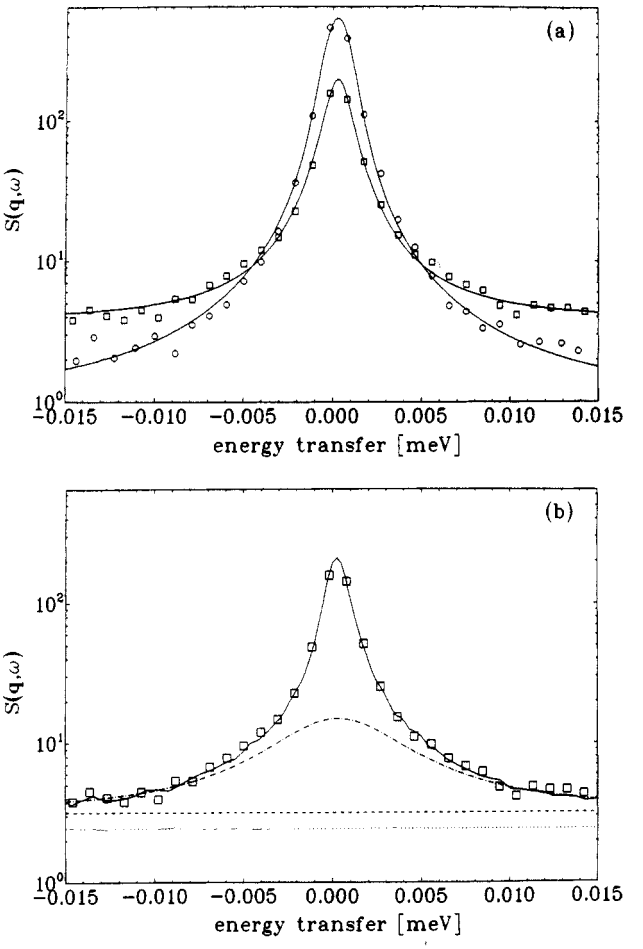

Figure 9. (a) Dynamic structure factor measured on IN10 for sample III at q = 1.71 Å^{-1} for T = 100 (○) and 320 K (□). (b) Representation of the 320 K data by eq 13.

to the Lorentzian with a much larger line width already detected in the IN13 measurements. The broad Lorentzian here shows up as a component with constant intensity. In the data representation we therefore assumed the following form of $S(q,\omega)$:

$$S(q,\omega) = \left[S_B + S_E(q)\,\delta(\omega) + S_{L1}(q)\frac{1}{\Pi(\Gamma_1/2)} + S_{L2}(q)\frac{1}{\Pi}\frac{\Gamma_2/2}{\omega^2 + (\Gamma_2/2)^2} \right] \otimes \phi_{10}(\omega) \quad (13)$$

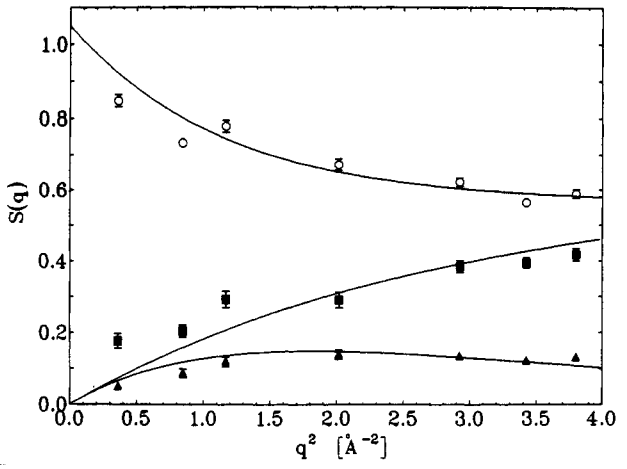

Figure 10. Sample III, $T = 275$ K. Structure factors associated with the elastic part (○), the broad quasielastic line (■), and the narrow quasielastic line (▲).

Again one can make use of the requirement that the integral intensity does not change, which means

$$S_E + S_{L1} + S_{L2} = 1 \tag{14}$$

The background scattering S_B is assumed as temperature independent and is taken from the low-temperature measurement; $\phi_{10}(\omega)$ denotes the instrumental resolution function of IN10. The fit yields for the structure factors the values

$$S_E = 0.33, \quad S_{L2} = 0.12, \quad S_{L1} = 0.55$$

and for the relaxation rates of the two processes the values

$$\Gamma_1 = 0.54 \text{ meV}, \quad \Gamma_2 = 7\ \mu\text{eV}$$

Of course, given only part of the spectrum in the restricted energy range of the instrument, the derived values can only be approximate. Clear, however, becomes the fact that the motion is made up of two different contributions, one with a relaxation rate on the order of about μeV and the other much larger, on the order of 0.1–1 meV.

Figure 10 shows the q dependence of the three structure factors S_E, S_{L1}, and S_{L2} for $T = 275$ K. They can be described, proceeding further from eqs 11 and 12 including the second quasielastic process, by

$$S_E(q) = \alpha + (1-\alpha)\exp[-(\langle u^2\rangle_{r1} + \langle u^2\rangle_{r2})q^2/3)] \tag{15}$$

$$S_{L1}(q) = (1-\alpha)(1-\exp[-(\langle u^2\rangle_{r1}q^2/3)]) \tag{16}$$

$$S_{L2}(q) = (1-\alpha)\exp[-(\langle u^2\rangle_{r1}q^2/3)](1-\exp[-\langle u^2\rangle_{r2}q^2/3)] \tag{17}$$

A representation of the data by these equations yields the displacements of the two processes, $\langle u^2\rangle_{r1}$ and $\langle u^2\rangle_{r2}$, separately. The corresponding curves, following from the data fit, are given in Figure 10. The values obtained are

$$\langle u^2\rangle_{r1} = 1.35 \text{ Å}^2 \qquad \langle u^2\rangle_{r2} = 1.40 \text{ Å}^2$$

It is interesting to compare the displacements determined by the decomposition of the dynamic structure factor with those derived from the fixed-window scans, Figure 11 shows a comparison between the sum of $\langle u^2\rangle_{r1}$ and $\langle u^2\rangle_{r2}$ with $\langle u^2\rangle_r$. The agreement is satisfactory. Figure 12 presents separately the temperature dependences of the displacements associated with the slow and the rapid process. It shows in addition the sum of the displacements and the

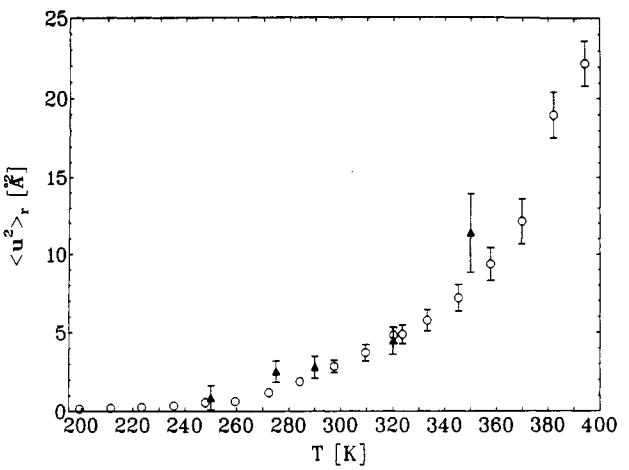

Figure 11. Temperature dependence of the diffusive displacements in sample III, obtained using IN10. Comparison of the results of the fixed-window scans (○) with the values $\langle u^2\rangle_r = \langle u^2\rangle_{r1} + \langle u^2\rangle_{r2}$ derived from the spectral decomposition (▲).

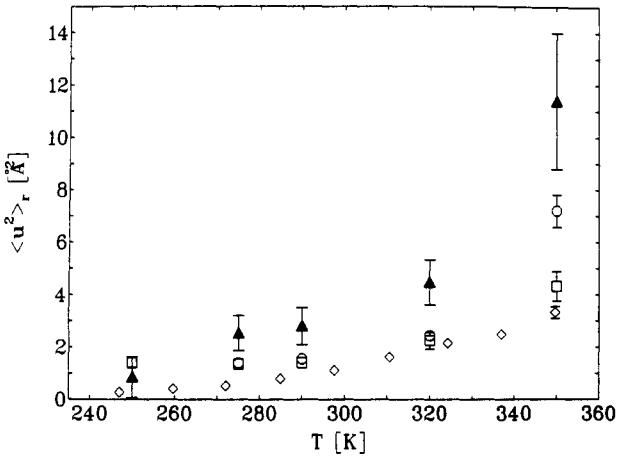

Figure 12. Temperature dependence of the diffusive displacements in sample III: rapid process with $\langle u^2\rangle_{r1}$ (□), slow process with $\langle u^2\rangle_{r2}$ (○), total displacement $\langle u^2\rangle_r$ (▲), displacement derived from IN13 fixed-window scan (◇).

displacements measured on IN13, the instrument with the lower energy resolution. The general impression is that the slow and the rapid process contribute with similar weights to the total displacement up to 320 K. Melting, which becomes quite pronounced at the higher temperatures seems to affect mainly the slow process. As expected, the measurement on IN13 only detects the rapid process; the slow process remains hidden in the elastic line.

Figure 13 finally shows the q dependence of the relaxation frequencies Γ_1 (for 250 and 275 K) and Γ_2 (for 275 K). Both appear to be independent of q. The values derived for Γ_1 are quite similar to those obtained in the IN13 experiment on sample I. Again one notes an increase of Γ_1 with temperature.

Discussion. Incoherent quasielastic neutron scattering experiments on polyethylene melts at temperatures above 415 K reported in a brief paper by Buchenau et al.[9] have already indicated the occurrence of a quasielastic central line with a half-width in the range 0.5–1 meV. The observed q dependence of the intensity suggested displacements of ~1.5 Å. Our measurements, which were conducted at lower temperatures, confirm these first observations. They show in addition that this motion sets in around T_g, at first with a lower relaxation rate, which then increases up to the value found in the melt (Figures 7 and 12a). We found that the mode is fully activated at

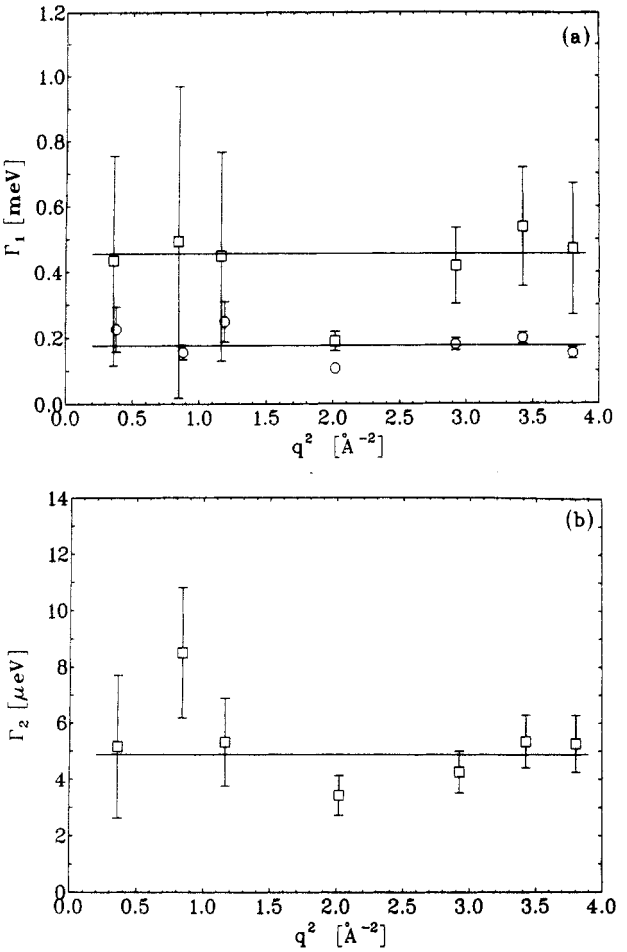

Figure 13. Sample III: q dependence of the relaxation rates of (a) the rapid process at T = 250 (○) and 275 K (□) and (b) the slow process at T = 275 K.

temperatures above ~320 K and then produces displacements $\langle u^2 \rangle_{r1} \simeq 2$ Å^2, in agreement with Buchenau's result cited above.

Similar modes, with energy transfers on the order of 0.5–2 meV, have already been observed in studies on other polymeric and low molecular weight glass-forming liquids.[10-13] Since these modes always become activated around T_g, their occurrence might constitute a basic feature of the glass transition. The microscopic character of the mode is not yet clear; it might be an overdamped vibration or a jump process between different conformational states. In any case, the process is localized and possesses, after an initial stage, an essentially constant correlation time.

It is a reasonable assumption to associate the slow process with relaxation rates Γ_2 with the usual segmental diffusion. In a mechanical relaxation experiment it is reflected in the β- and γ-processes. In the frequency range of the experiment (GHz) the β- and γ-processes show similar rates. At higher frequencies they merge together and become identical; at lower frequencies they separate. The observed behavior is that expected just for the range where the separation point is located. For temperatures below 320 K, we observe an essentially constant displacement $\langle u^2 \rangle_{r2} \simeq 2$ Å^2 and a weak temperature dependence of the relaxation rates (the estimated activation energy is ~10 kJ/mol). These are properties as are expected for the γ-process, usually associated with a localized kink movement.[14] For higher temperatures, however, in the range of pronounced partial melting, the displacement $\langle u^2 \rangle_{r2}$ further increases, showing values which cannot be explained by a local kink motion. It appears that here the motion becomes more β-like, with diffusive displacements over larger distances. Since the frequency of the spectrometer is unchanged, we must conclude that the bifurcation point, where the β-process separates from the γ-process, shifts as a result of partial melting. This appears principally possible, since the release of the constraints in the disordered regions resulting from the surface melting changes in fact the structure.

Acknowledgment. Support of this work by Ministerium für Forschung und Technologie, Bonn, Germany and the Institut Laue-Langevin, Grenoble, France is gratefully acknowledged.

References and Notes

(1) Tanabe, Y.; Strobl, G. R.; Fischer, E. W. *Polymer* **1986**, *27*, 1147.
(2) Strobl, G. R. In *Non-Crystalline Solids*; Conde, A., Ed.; *World Scientific Publishing Co.*: London, 1992; in press.
(3) Springer, T. *Quasielastic Neutron Scattering for the Investigation of Diffusive Motions in Solids and Liquids*; Springer: Berlin, 1972.
(4) Strobl, G. *J. Polym. Sci., Polym. Symp. Ed.* **1977**, *59*, 121.
(5) Mutter, R.; Strobl, G., to be published in *J. Polym. Sci., Polym. Phys. Ed.*
(6) Fischer, E. W. *Kolloid Z. Z. Polym.* **1967**, *218*, 97.
(7) Zachmann, H. G. *Kolloid Z. Z. Polym.* **1969**, *231*, 504.
(8) Rieger, J.; Mansfield, M. L. *Macromolecules* **1989**, *22*, 3810.
(9) Buchenau, U.; Monkenbusch, M.; Stamm, M.; Majkrzak, C. F.; Nücker, N. In *Polymer Motion in Dense Systems*; Richter, D., Springer, T., Eds.; Springer: Berlin, 1988; p 138.
(10) Frick, B.; Richter, D.; Petry, W.; Buchenau, U. *Z. Phys. B* **1988** *70*, 73.
(11) Fujara, F.; Petry, W. *Europhys. Lett.* **1987**, *4*, 921.
(12) Bartsch, E.; Fujara, F.; Kiebel, M.; Sillescu, H.; Petry, W. *Ber. Bunsen-Ges. Phys. Chem.* **1989**, *93*, 1252.
(13) Kanaya, T.; Kaji, K.; Inoue, K. *Macromolecules* **1991**, *24*, 1826.
(14) Pechhold, W. *Kolloid Z. Z. Polym.* **1968**, *228*, 1.

Registry No. Polyethylene, 9002-88-4; neutron, 12586-31-1.